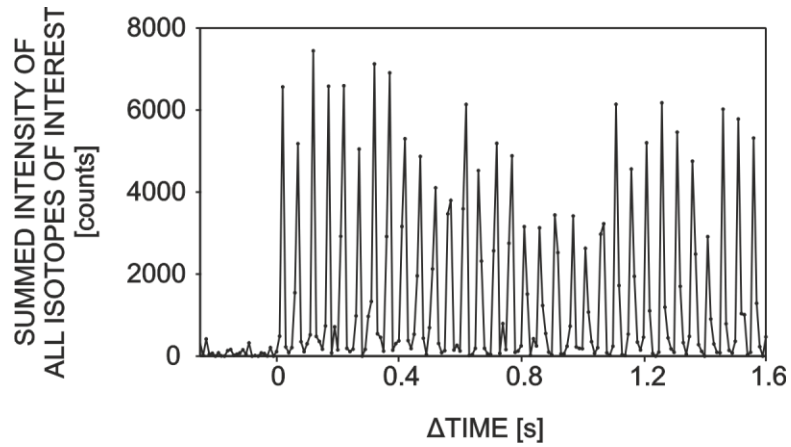


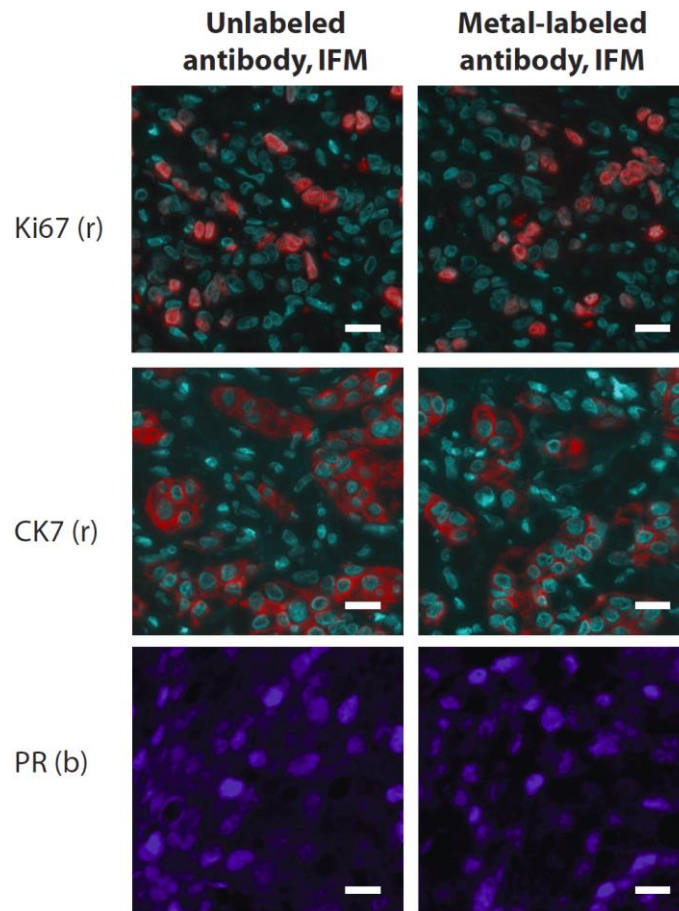
SUPPLEMENTARY FIGURES

Supplementary Fig. 1 | Signal separation of ablation chamber at 20 Hz.



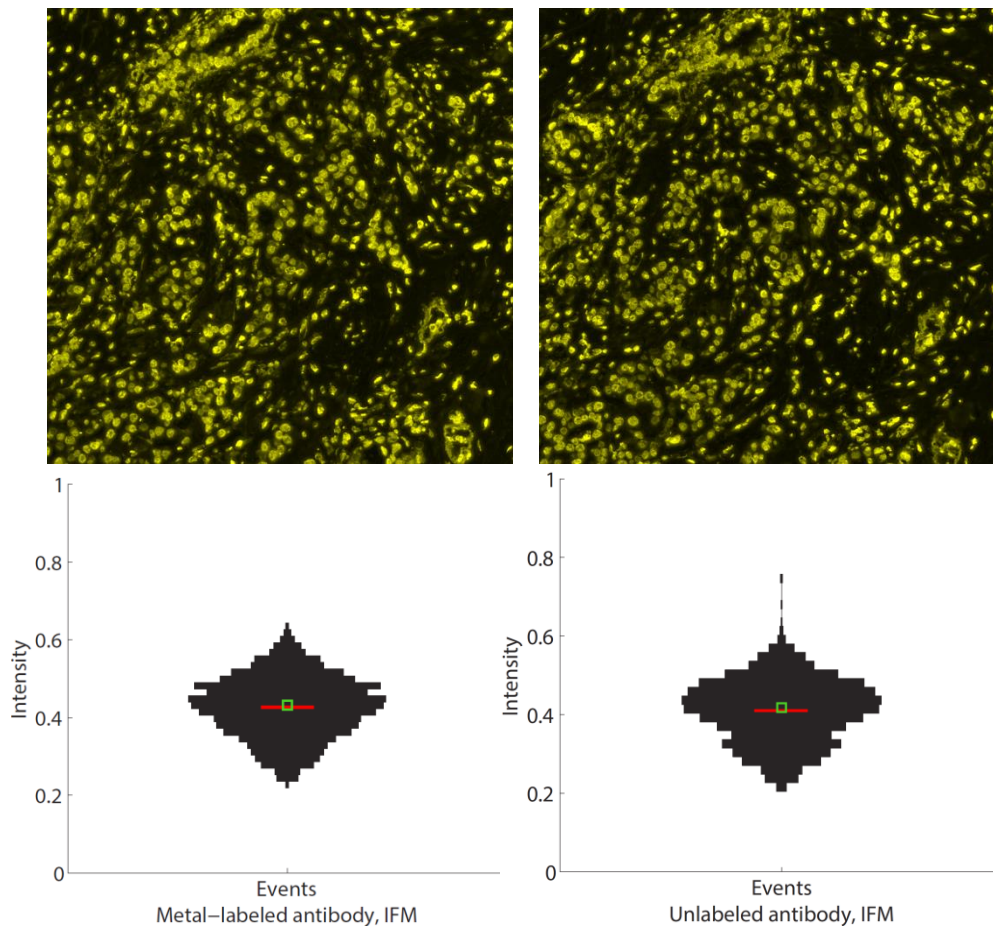
The shown signal was summed over all measured channels. A clear separation of signal is observed between individual laser shots.

Supplementary Fig. 2 | Validation of the approach, comparison between unlabeled and metal-labeled antibodies by IFM.



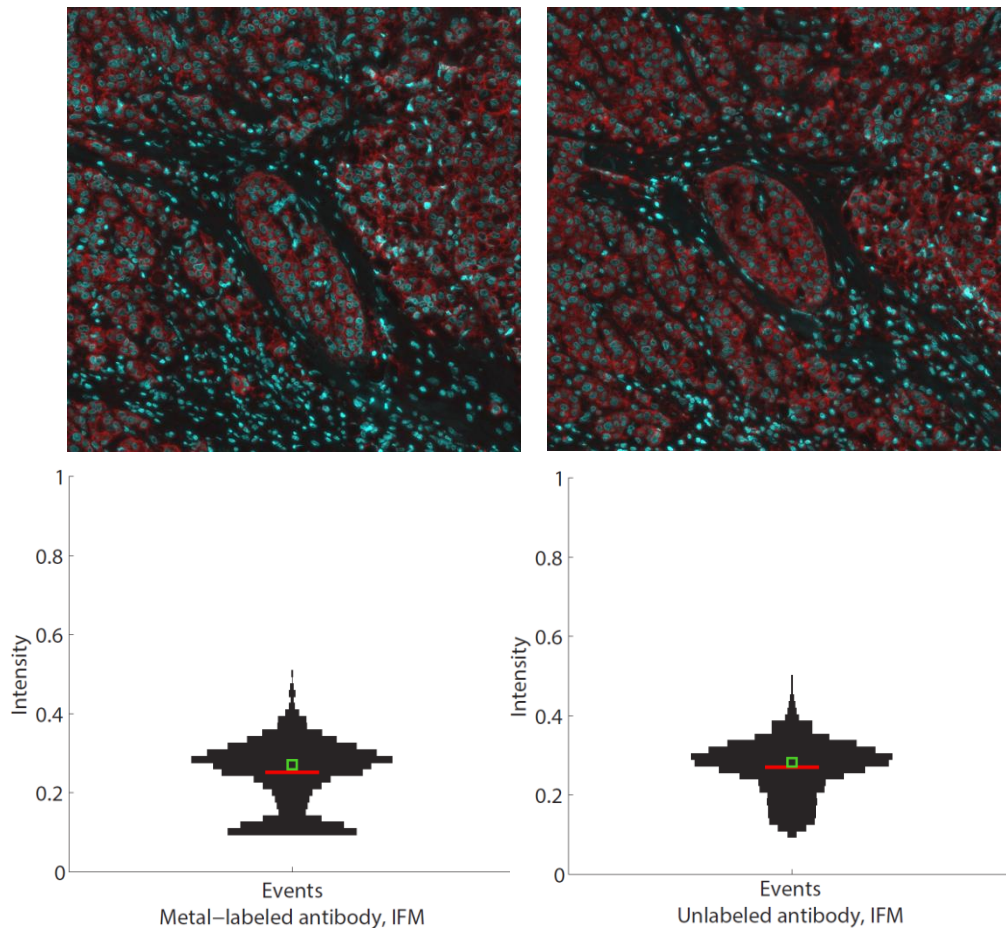
The specificity of unlabeled (stock) and metal-labeled antibodies was compared on breast cancer tissue sections of the Luminal HER2⁺ subtype (tissue no. 37) by IFM. The quantitative analysis of cytokeratin 7 is shown in Supplementary Fig. 3f. Hoechst 33258 is shown in cyan. No apparent changes in specificity were found. b = blue, r = red. The white size bars in the images indicate 25 μm .

Supplementary Fig. 3 | Comparison of single-cell signal intensities between metal-labeled and unlabeled antibodies by IFM.



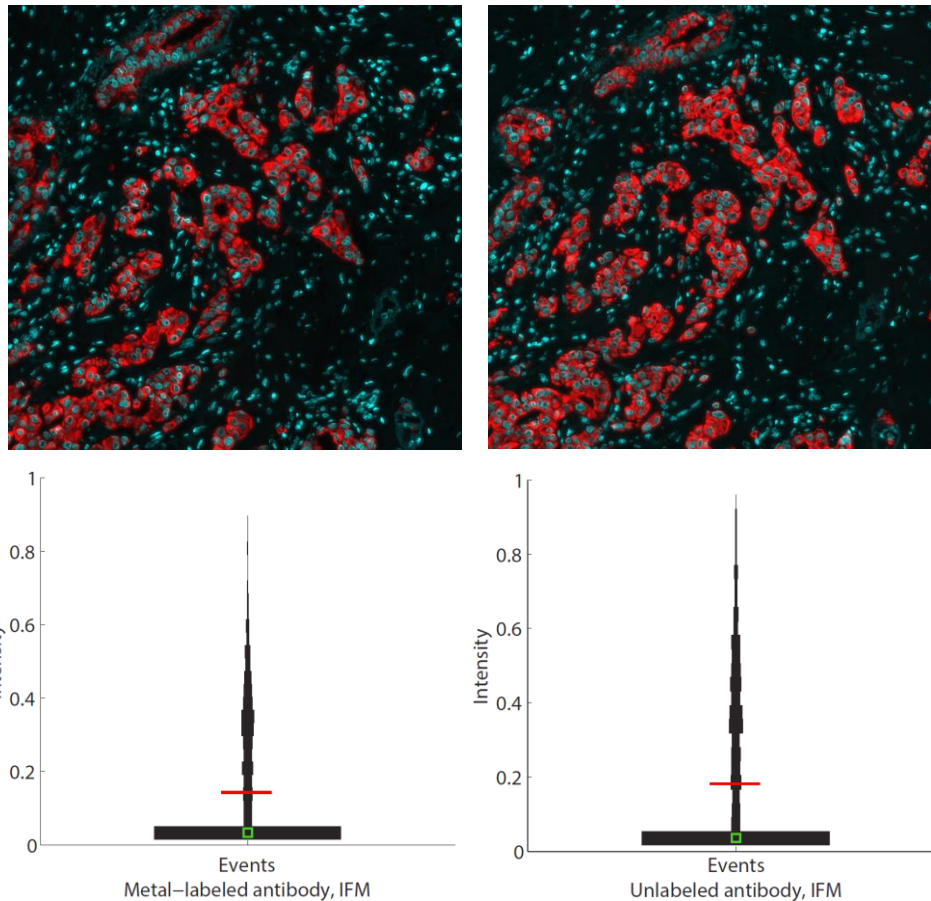
(a) IFM images of metal-labeled (top left image, $n = 1,559$) and unlabeled antibody (top right image, $n = 1,610$) against H3 on serial sections of case no. 37 are shown. These images were used to quantitatively compare single-cell signal intensities. The single-cell intensity distributions of the IFM analysis of the metal-labeled antibody (bottom left) and the unlabeled antibody (bottom right) are comparable. Event numbers were not normalized. The mean signal (red line) is 7 % higher in the IFM analysis of the metal-labeled antibody. The median signal is represented by the green square.

Supplementary Fig. 3 | Comparison of single-cell signal intensities between metal-labeled and unlabeled antibodies by IFM.



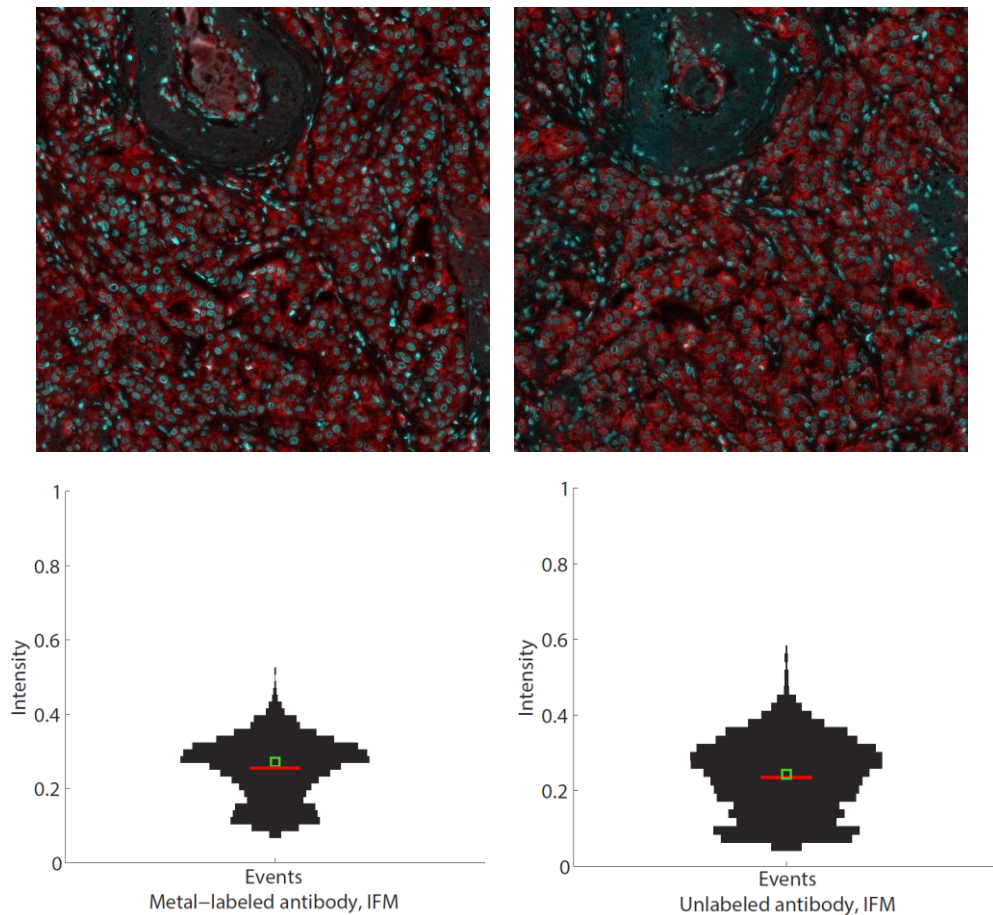
(b) IFM images of metal-labeled (top left image, $n = 2,066$) and unlabeled antibody (top right image, $n = 1,893$) against HER2 on serial sections of case no. 37 are shown. These images were used to quantitatively compare single-cell signal intensities. The single-cell intensity distributions of the IFM analysis of the metal-labeled antibody (bottom left) and the unlabeled antibody (bottom right) are comparable. Event numbers were not normalized. The mean signal (red line) is 7 % higher in the IFM analysis of the unlabeled antibody. The median signal is represented by the green square.

Supplementary Fig. 3 | Comparison of single-cell signal intensities between metal-labeled and unlabeled antibodies by IFM.



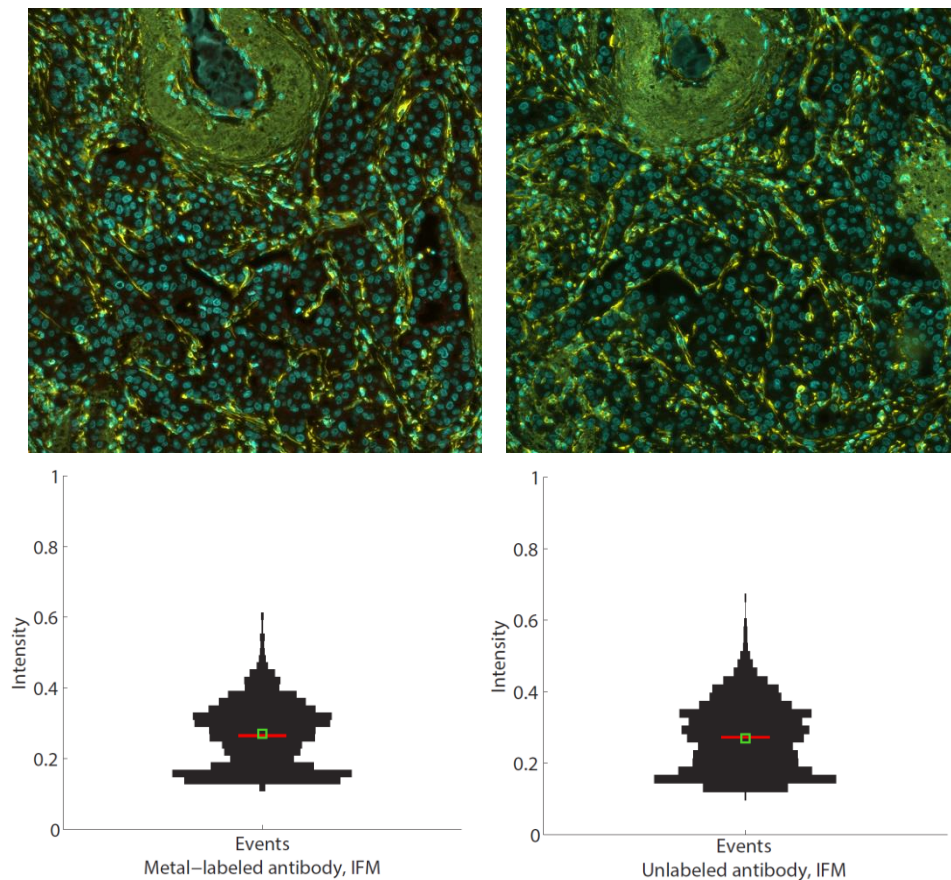
(c) IFM images of metal-labeled (top left image, $n = 1,523$) and unlabeled antibody (top right image, $n = 1,483$) against cytokeratin 8/18 on serial sections of case no. 37 are shown. These images were used to quantitatively compare single-cell signal intensities. The single-cell intensity distributions of the IFM analysis of the metal-labeled antibody (bottom left) and the unlabeled antibody (bottom right) are comparable. Event numbers were not normalized. The mean signal (red line) is 27 % higher in the IFM analysis of the unlabeled antibody. The median signal is represented by the green square.

Supplementary Fig. 3 | Comparison of single-cell signal intensities between metal-labeled and unlabeled antibodies by IFM.



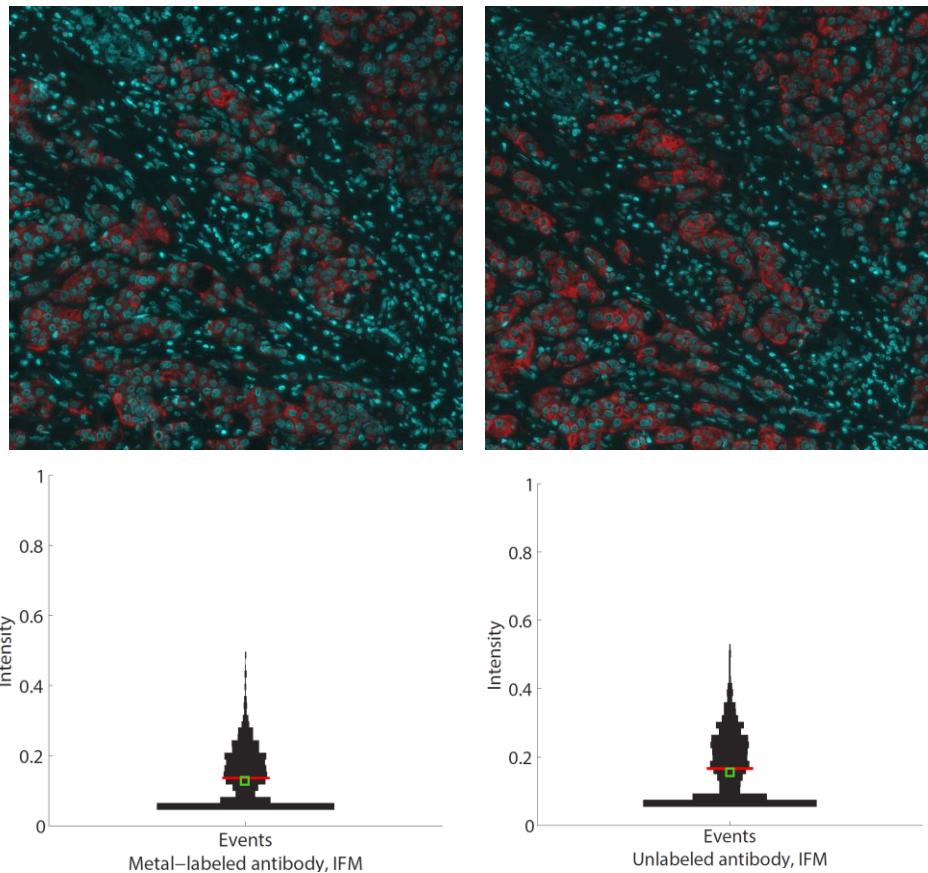
(d) IFM images of metal-labeled (top left image, $n = 1,304$) and unlabeled antibody (top right image, $n = 2,458$) against E-cadherin on serial sections of case no. 37 are shown. These images were used to quantitatively compare single-cell signal intensities. The single-cell intensity distributions of the IFM analysis of the metal-labeled antibody (bottom left) and the unlabeled antibody (bottom right) are comparable. Event numbers were not normalized. The mean signal (red line) is 7 % higher in the IFM analysis of the unlabeled antibody. The median signal is represented by the green square.

Supplementary Fig. 3 | Comparison of single-cell signal intensities between metal-labeled and unlabeled antibodies by IFM.



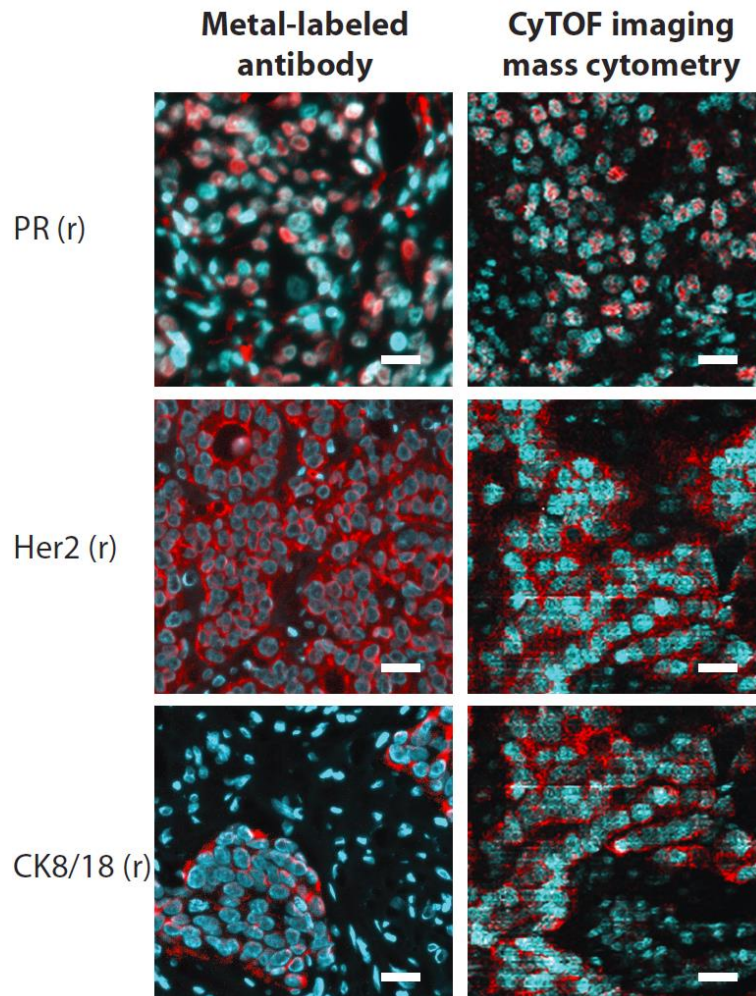
(e) IFM images of metal-labeled (top left image, $n = 2,331$) and unlabeled antibody (top right image, $n = 2,460$) against vimentin on serial sections of case no. 37 are shown. These images were used to quantitatively compare single-cell signal intensities. The single-cell intensity distributions of the IFM analysis of the metal-labeled antibody (bottom left) and the unlabeled antibody (bottom right) are comparable. Event numbers were not normalized. The mean signal (red line) is 2 % higher in the IFM analysis of the metal-labeled antibody. The median signal is represented by the green square.

Supplementary Fig. 3 | Comparison of single-cell signal intensities between metal-labeled and unlabeled antibodies by IFM.



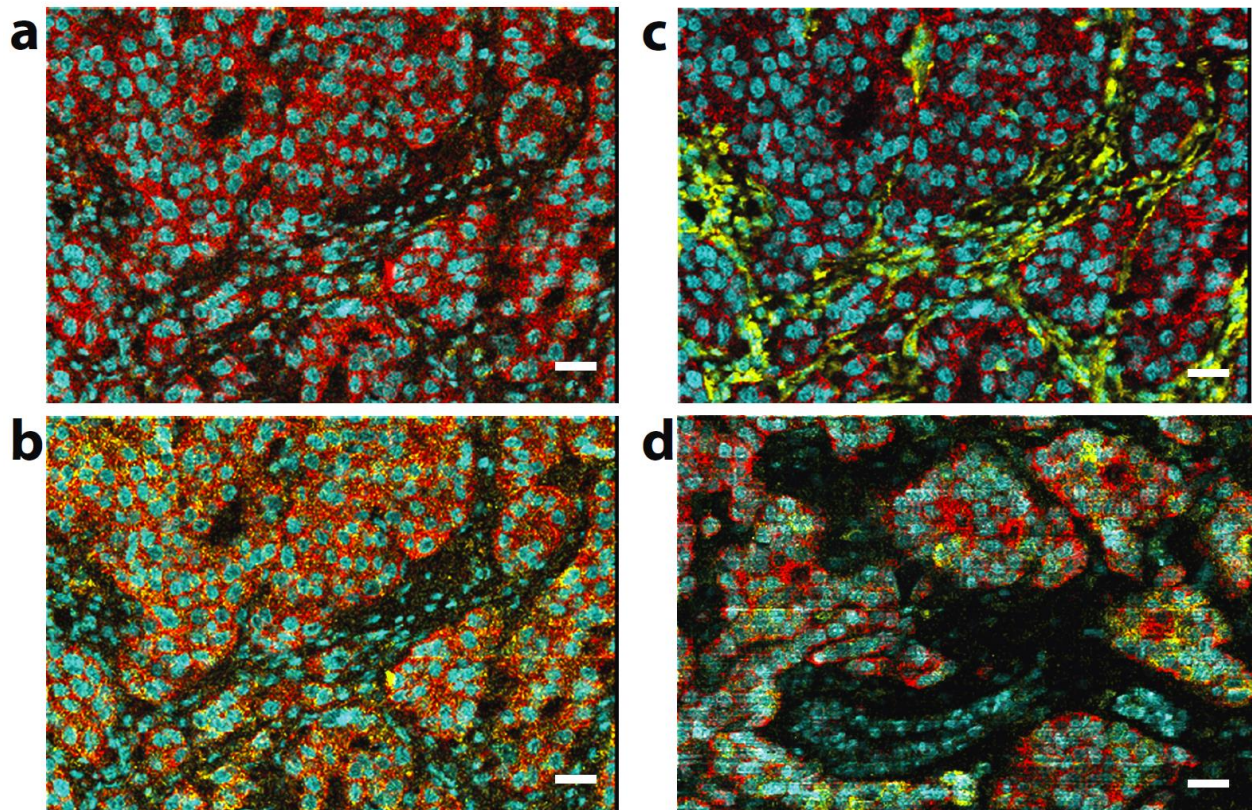
(f) IFM images of metal-labeled (top left image, $n = 1,958$) and unlabeled antibody (top right image, $n = 2,000$) against cytokeratin 7 on serial sections of case no. 37 are shown. These images were used to quantitatively compare single-cell signal intensities. The single-cell intensity distributions of the IFM analysis of the metal-labeled antibody (bottom left) and the unlabeled antibody (bottom right) are comparable. Event numbers were not normalized. The mean signal (red line) is 22 % higher in the IFM analysis of the unlabeled antibody. The median signal is represented by the green square.

Supplementary Fig. 4 | Comparison between IFM and CyTOF imaging mass cytometry.



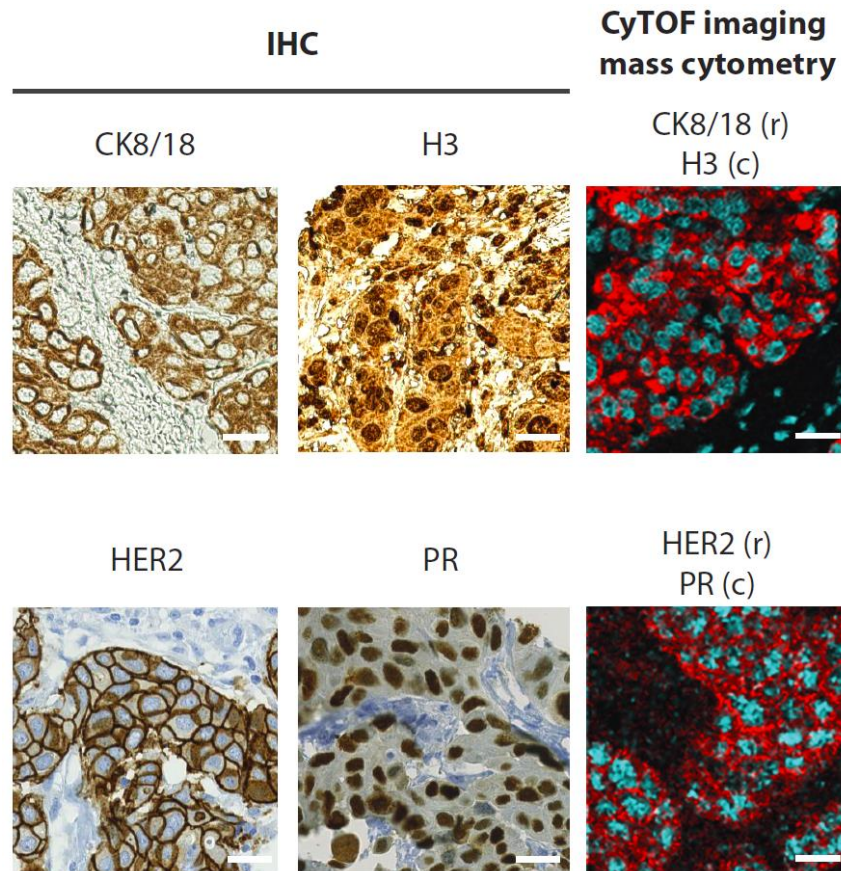
The specificity of metal-labeled antibodies analyzed by IFM and by CyTOF imaging mass cytometry was compared on breast cancer tissue sections of the Luminal HER2⁺ subtype (PR case no. 210, HER2 and cytokeratin 8/18 case no. 23). Hoechst 33258 and H3 are shown in cyan and the listed markers in red. No apparent changes in specificity were found. The scale maxima indicating the counts per laser shot were adjusted as follows: H3, 200 (case no. 210) and 400 (case no. 23); PR, 10; HER2, 50; cytokeratin 8/18, 30. The white size bars in the images indicate 25 μm.

Supplementary Figure 5 | Representative breast cancer tissue imaging mass cytometry images.



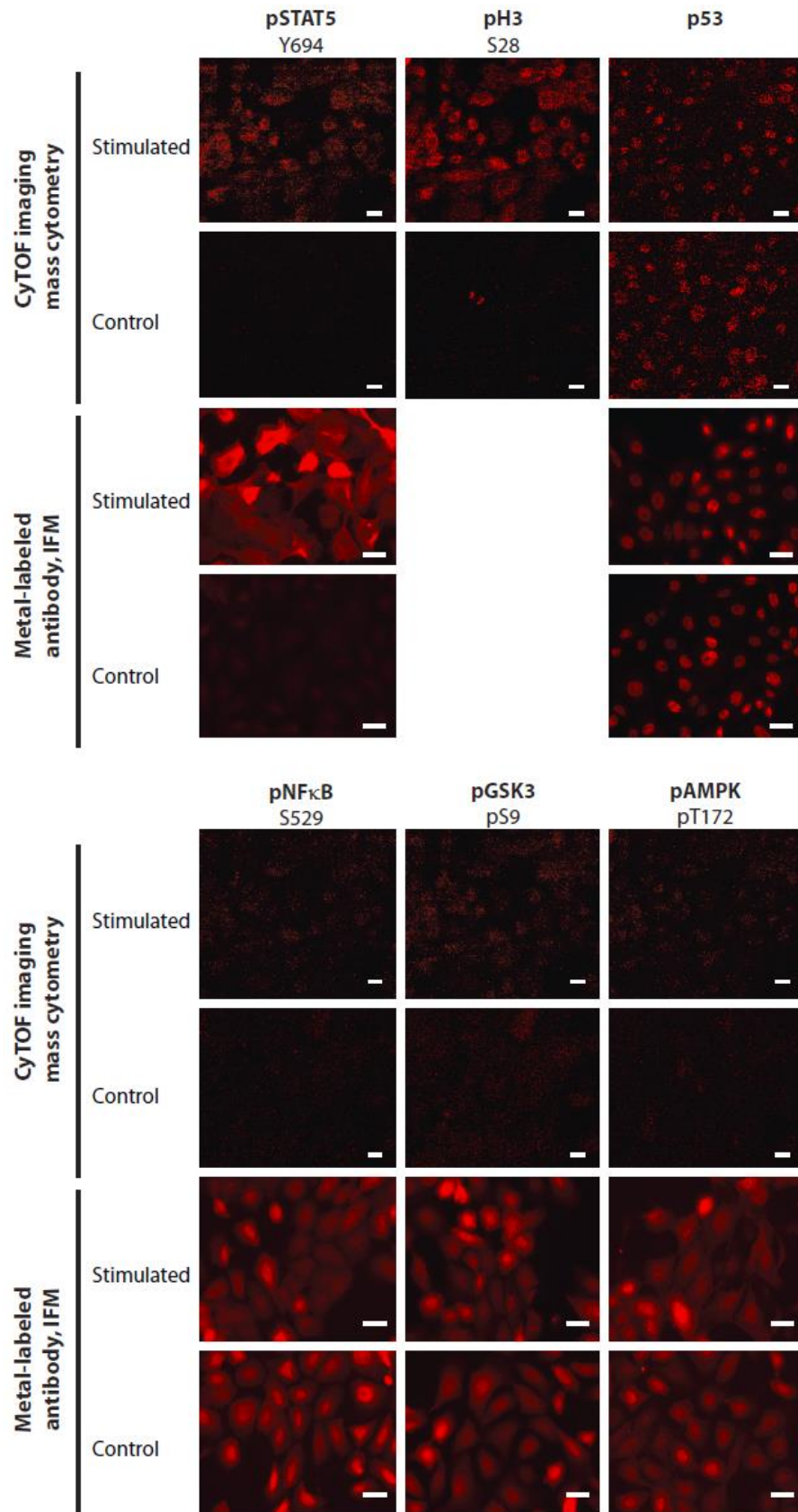
(a) Image of tissue no. 210 showing overlay of β -catenin (red), H3 (cyan), and pS6 (yellow). **(b)** Image of tissue no. 210 showing overlay of HER2 (red), H3 (cyan), and CAH IX (yellow). **(c)** Image of tissue no. 210 showing overlay of E-cadherin (red), H3 (cyan), and vimentin (yellow). **(d)** Image of tissue no. 23 showing overlay of cytokeratin 8/18 (red), H3 (cyan), and phosphorylation on S6 (yellow). A total of 32 proteins and protein phosphorylation sites were measured simultaneously at 1 μm resolution (Fig. 3, Supplementary Tables 1 and 2). The scale maxima indicating the counts per laser shot were adjusted as follows: pS6, 15 (tissue no. 210) and 20 (tissue no. 23); H3, 200 (tissue no. 210) and 400 (tissue no. 23); β -catenin, 20; HER2, 30; CAH IX, 15; E-Cadherin, 20; vimentin, 400; Cytokeratin 8/18, 25. The white size bars in the images indicate 25 μm .

Supplementary Fig. 6 | Comparison between single-plex IHC and 32-plex imaging mass cytometry measurements.



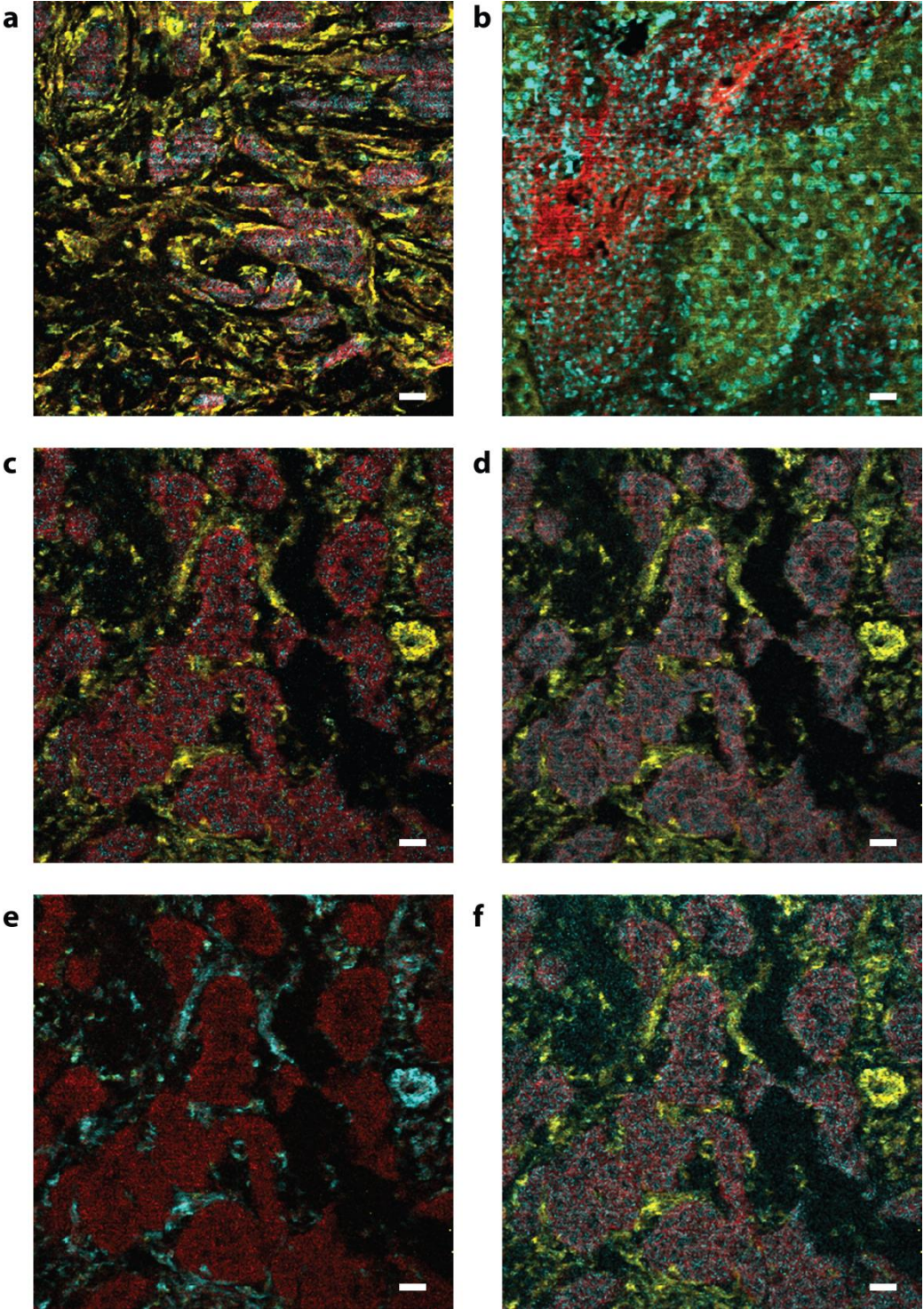
Sections of the same Luminal HER2⁺ tumor were used (case no. 210), but sections were *not* serial. No apparent difference in staining pattern was found. The scale maxima indicating the counts per laser shot were adjusted as follows: HER2, 30; PR, 10; CK8/18, 80; H3, 200. The white size bars in the images indicate 25 μ m. For the upper row, the same antibody clones for the imaging mass cytometry and IHC analysis were used. For the bottom row, different antibody clones for the imaging mass cytometry and IHC analysis were used (imaging mass cytometry: HER2, BD (3B5); PR, Epitomics (EP2) and IHC: HER2, Ventana (4B5); PR, Ventana (1E2)).

Supplementary Fig. 7 | Imaging mass cytometry analysis of HMLE cells.



Analysis of phosphorylation on NF κ B, GSK3, AMPK, STAT5, and H3 before and after a 30-min stimulation with the tyrosine phosphatase inhibitor vanadate. Analysis of p53 is also shown. For each control and stimulation comparison the experimental conditions and image processing settings were kept constant. The scale maxima indicating the counts per laser shot were adjusted as followed: p53, 30; pNF κ B, 30; pGSK3, 30; pAMPK, 30; pSTAT5, 60; pH3, 60; CD44, 200. The white size bars in the images indicate 25 μ m. Of note, for imaging mass cytometry a primary antibody stain was used for detection, whereas in IFM a secondary antibody stain was used for detection. The latter will increase the sensitivity of the detection. For pH3 no immunofluorescence images were available.

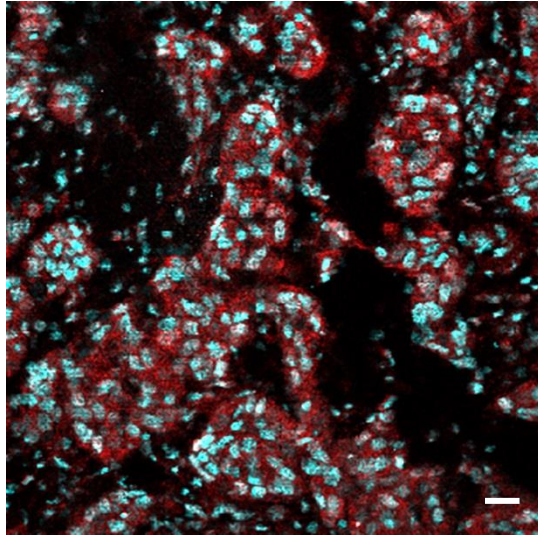
Supplementary Fig. 8 | Example images showing marker expression for a given SPADE subpopulation.



Example images showing marker expression used for SPADE clustering. The scale maxima indicating the counts per laser shot are shown after each marker. **(a)** tumor case no. 79 pERK (red, 100), pAMPK (cyan, 100), Vimentin (yellow, 1000). **(b)** tumor case no. 201 CD20 (red, 200), H3 (cyan, 300), E-Cadherin (yellow, 300). **(c)** tumor case no. 210 HER2 (red, 200), Caspase3 (cyan, 20), Vimentin (yellow, 500). **(d)** tumor case no. 210 HER2 (red, 200), ER (cyan, 80), Vimentin (yellow, 500). **(e)** tumor case no. 210 pBad (red, 50), Vimentin (cyan, 500), CD68 (yellow, 60). **(f)** tumor case no. 210 HER2 (red, 200), PR (cyan, 20), Vimentin (yellow, 500).

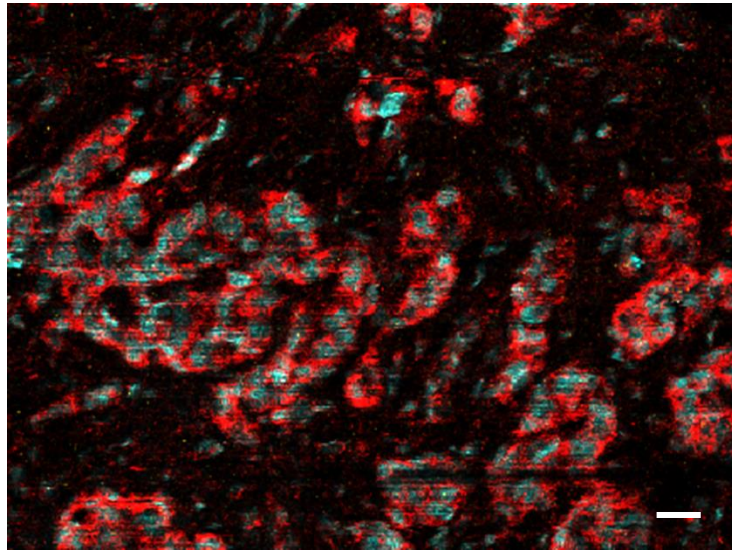
Other markers used for SPADE clustering are shown in: c-MYC Supplementary Fig. 9; H3 Supplementary Fig. 9, Supplementary Fig. 10a, Supplementary Fig. 11b-c, Supplementary Fig. 5a-d, Supplementary Fig. 6, Fig. 3a,b,d, Fig. 2b; HER2 Supplementary Fig. 10a, Supplementary Fig. 12a-c, Supplementary Fig. 4, Supplementary Fig. 5b, Supplementary Fig. 6, Fig. 3d, Fig. 2b; CK8/18 Supplementary Fig. 10a, Supplementary Fig. 4, Supplementary Fig. 5d, Supplementary Fig. 6, Fig. 3a, Fig. 2b; CAH IX Supplementary Fig. 11b-c, Supplementary Fig. 5b; Vimentin Supplementary Fig. 11b-c, Supplementary Fig. 12a-b, Supplementary Fig. 5c, Fig. 3a,d, Fig. 2b; pS6 Supplementary Fig. 12a-c, Supplementary Fig. 5a,d, Fig. 3e; PR Supplementary Fig. 4, Supplementary Fig. 6, Fig. 3c; β -catenin Supplementary Fig. 5a, Fig. 3f; E-Cadherin Supplementary Fig. 5c, Fig. 3e, Fig. 2b, CK7 Fig. 3b, e; CD44 Fig. 3b; CD68 Fig. 3c,f; ER Fig. 3f; pS6 Fig. 3e, Supplementary Fig. 5a, d, Supplementary Fig. 12a-c.

Supplementary Fig. 9 | Imaging mass cytometry image of tumor no. 210.



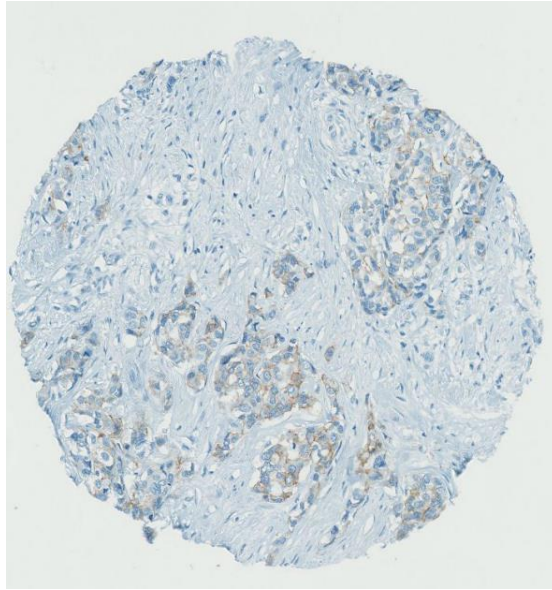
Expression of c-MYC (red) and H3 (cyan) in tumor case no. 210 determined by imaging mass cytometry. The scale maxima indicating the counts per laser shot were adjusted as followed: c-Myc, 150; H3, 400. The white size bar in the image indicates 25 μm .

Supplementary Fig. 10 | Imaging mass cytometry analysis of tumor no. 162.



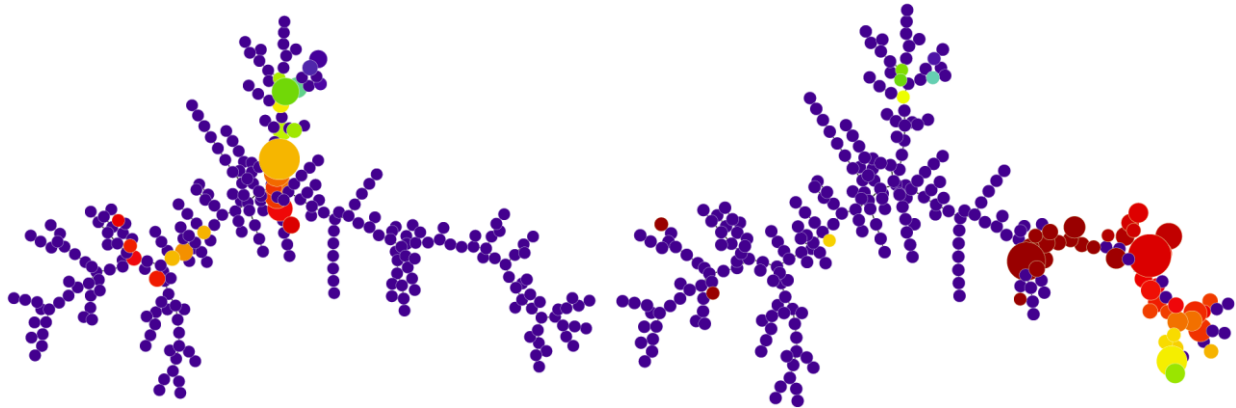
(a) HER2 (red), H3 (cyan), and cytokeratin 8/18 (yellow) staining of the Triple-negative tumor no. 162 by imaging mass cytometry is shown. The scale maxima indicating the counts per laser shot were adjusted as followed: HER2, 50; H3, 200; cytokeratin 8/18, 50. The white size bar in the image indicates 25 μm .

Supplementary Fig. 10 | Imaging mass cytometry analysis of tumor no. 162.



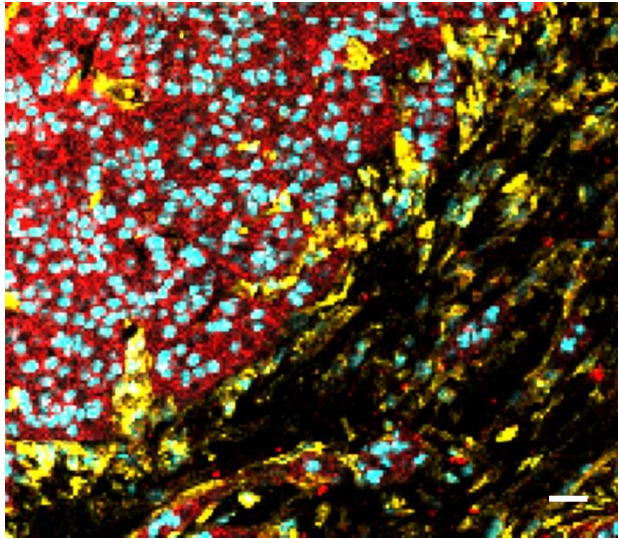
(b) HER2 stain of the Triple-negative tumor no. 162 analyzed by IHC. The anti-HER2 antibody used for routine IHC TMA staining was a different clone (4B5, Ventana) than the antibody used for imaging mass cytometry (3B5, Becton Dickinson (BD)); both antibodies yield the same HER2 staining levels (Supplementary Fig. 6).

Supplementary Fig. 11 | Analysis of CAH IX expression in breast cancer by SPADE



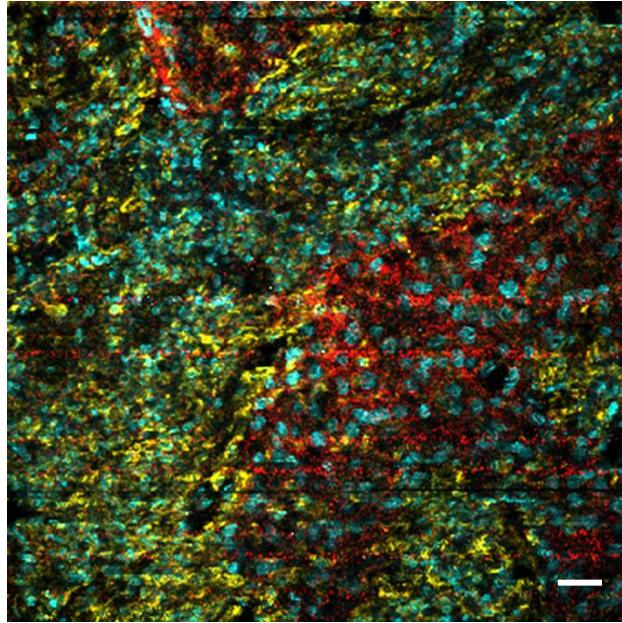
(a) Tumor cases no. 260 (left) and no. 201 (right) are shown. The color scale indicates the expression of CAH IX, and the size of the nodes shows the percentage of cells for a given cluster of this tumor.

Supplementary Fig. 11 | Analysis of CAH IX expression in breast cancer by SPADE



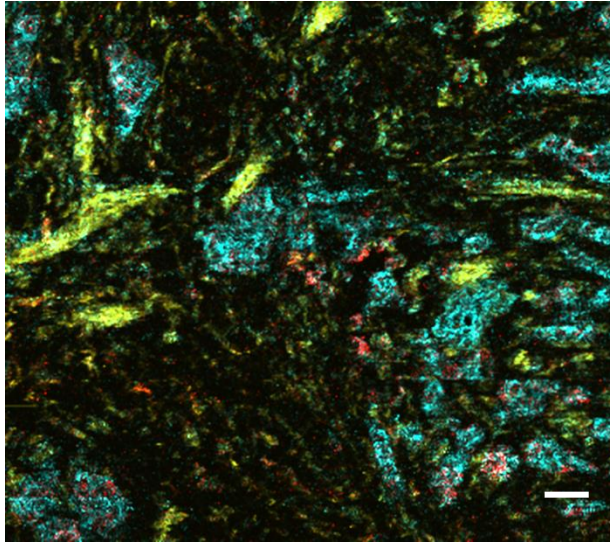
(b) Staining of CAH IX (red), H3 (cyan), and vimentin (yellow) on tumor no. 260 analyzed by imaging mass cytometry. The scale maxima indicating the counts per laser shot were adjusted as followed: CAH IX, 100; H3, 700; vimentin, 300. The white size bar in the image indicates 25 μm .

Supplementary Fig. 11 | Analysis of CAH IX expression in breast cancer by SPADE



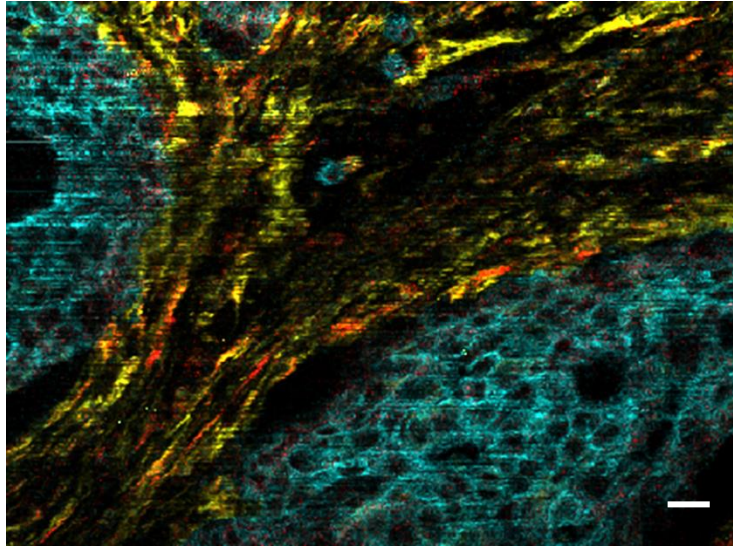
(c) Expression of CAH IX (red), H3 (cyan), and vimentin (yellow) on tumor no. 201 analyzed by imaging mass cytometry. The scale maxima indicating the counts per laser shot were adjusted as followed: CAH IX, 70; H3, 300; vimentin, 200. The white size bars in the image indicate 25 μm .

Supplementary Fig. 12 | Analysis of pS6 level in breast cancer by SPADE



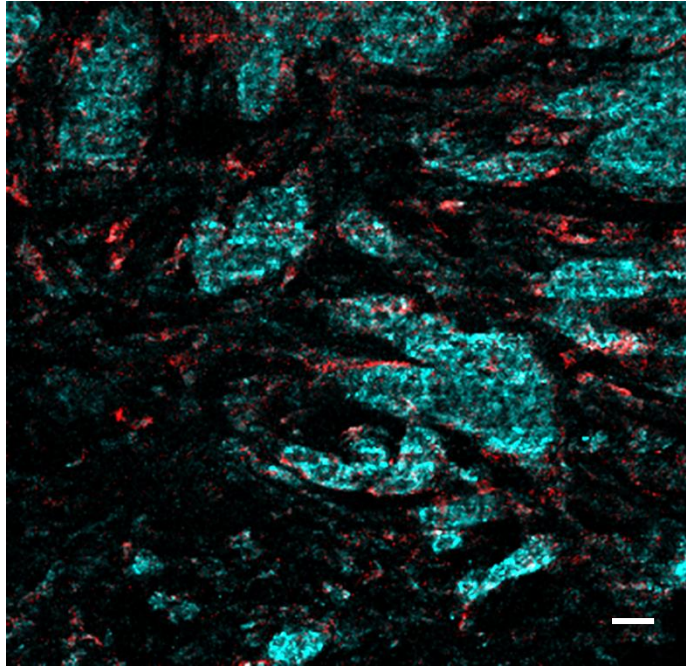
(a) Level of pS235/pS236 on S6 (red) and expression of total HER2 (cyan) and vimentin (yellow) on tumor no. 168 were analyzed by imaging mass cytometry. The scale maxima indicating the counts per laser shot were adjusted as followed: pS6, 60; HER2, 100; vimentin, 600. The white size bar in the image indicates 25 μm .

Supplementary Fig. 12 | Analysis of pS6 level in breast cancer by SPADE



(b) Levels of pS235/pS236 on S6 (red) and expression of total HER2 (cyan) and vimentin (yellow) on tumor no. 273 were determined by imaging mass cytometry. The scale maxima indicating the counts per laser shot were adjusted as followed: pS6, 60; HER2, 100; vimentin, 600. The white size bar in the image indicates 25 μm .

Supplementary Fig. 12 | Analysis of pS6 level in breast cancer by SPADE



(c) Levels of pS235/pS236 on S6 (red) and expression of total HER2 (cyan) on tumor no. 79 were analyzed by imaging mass cytometry. The scale maxima indicating the counts per laser shot were adjusted as followed: pS6, 60; HER2, 300. The white size bar in the image indicates 25 μm .

SUPPLEMENTARY TABLES

Supplementary Table 1 | Antibodies used for tumor case no. 23 (Fig. 2b, Fig. 3d-f and Supplementary Fig. 4).

Isotope	Antigen	Antibody raised against	Clone	Final conc. [$\mu\text{g/mL}$]	Supplier
139La	ER	Total, synthetic peptide within residues 200 - 300		5	Abcam
141Pr	PR	Residues surrounding Y541	D8Q2J	5	CST
142Nd	pSHP2	pY542		5	Abcam
143Nd	p53	Total	7F5	5	CST
144Nd	CD31	Total, surface	HC1/6	5	Millipore
145Nd	TWIST	Amino-terminal residues	ABD29	5	Millipore
146Nd	CD68	Total, surface	Y1/82A	5	Biolegend
147Sm	CD3	Total, surface	UCHT1	5	Biolegend
148Nd	SLUG	Total	C19G7	5	CST
149Sm	CD20	Total, surface	L26	5	eBioscience
150Nd	c-MYC	C-terminal domain	9 E10	5	Biolegend
151Eu	HER2 (ErbB-2)	C-terminal domain	3B5	5	BD
152Sm	pAMPK	pT172	40H9	5	CST
153Eu	pAKT	pS473	D9E	5	CST
154Gd	pERK1/2	pT202/ pY204	D13.14.4E	5	CST
156Gd	pNF κ B	pS536		5	Abcam
158Gd	pGSK3	pS9	5B3	5	CST
159Tb	pBAD	pS112	40A9	5	CST
160Gd	CD44	Total, surface	IM7	5	BD
162Dy	VIMENTIN	Total	D21H3	5	CST

164Dy	CK7	Total	RCK105	5	BD
165Ho	β -CATENIN	Total, when S33/S37/T41 are not phosphorylated	D13A1	5	CST
166Er	CAH IX	Total	AF2188	5	R&D Systems
167Er	E-CADHERIN	C-terminal residues	36/E-Cadherin	5	BD
168Er	Ki67	Total	B56	5	BD
169Tm	EGFR	Cytoplasmic domain	D38B1	5	CST
170Er	pS6	pS235/pS236	D57.2.2E	5	CST
171Yb	CD45	Total, surface	HI30	5	Biolegend
172Yb	CASPASE3	Cleaved@D175	5A1E	5	CST
174Yb	CK8/18	Total	C51	5	CST
175Lu	Pan-ACTIN	C-terminal domain	D18C11	5	CST
176Yb	H3	C-terminal domain	D1H2	5	CST

CST = Cell Signaling Technology, BD = Becton Dickinson. Community validation data for antibodies are given in Supplementary Note 1.

Supplementary Table 2 | Antibodies used for tumor case no. 210 (Fig. 2b, Fig. 3a-c and Supplementary Fig. 4).

Isotope	Antigen	Antibody raised against	Clone	Final conc. [$\mu\text{g/mL}$]	Supplier
139La	ZNF703	Synthetic peptide within amino acids 191-284	polyclonal	7.5	Abcam
141Pr	GATA3	Peptide between the trans-activation and DNA-binding domains	L50-823	7.5	BD
142Nd	pSHP2	pY542		7.5	Abcam
143Nd	p53	Total	7F5	7.5	CST
144Nd	CD31	Total, surface	HC1/6	7.5	Millipore
145Nd	TWIST	Amino-terminal residues	ABD29	7.5	Millipore
146Nd	CD68	Total, surface	Y1/82A	7.5	Biolegend
147Sm	CD3	Synthetic peptide: KAKAKPVTRGAGA, corresponding to amino acids 156-168 of human CD3 Epsilon chain	polyclonal	7.5	Abcam
148Nd	SLUG	Total	C19G7	7.5	CST
149Sm	CD20	Total, surface	L26	7.5	eBioscience
150Nd	c-MYC	C-terminal domain	9 E10	7.5	Biolegend
151Eu	HER2	C-terminal domain	3B5	7.5	BD

152Sm	pAMPK	pT172	40H9	7.5	CST
153Eu	pAKT	pS473	D9E	7.5	CST
154Gd	pERK1/2	pT202/pY204	D13.14.4E	7.5	CST
158Gd	PR	Synthetic peptide of residues near the N-terminus	EP2	7.5	Epitomics
159Tb	pBAD	pS112	40A9	7.5	CST
160Gd	CD44	Recombinant human CD44 Gln21-Pro220	polyclonal	7.5	R&D Systems
162Dy	VIMENTIN	Total	D21H3	7.5	CST
164Dy	CK7	Total	RCK105	7.5	BD
165Ho	β -CATENIN	Total, when S33/S37/T41 are not phosphorylated	D13A1	7.5	CST
166Er	CAH IX	Total	AF2188	7.5	R&D Systems
167Er	E-CADHERIN	C-terminal residues	36/E-Cadherin	7.5	BD
168Er	Ki67	Total	8D5	7.5	CST
169Tm	EGFR	Cytoplasmic domain	D38B1	7.5	CST
170Er	pS6	pS235/pS236	D57.2.2E	7.5	CST
171Yb	CD45	Total, surface	2B11	7.5	eBioscience
172Yb	CASPASE3	Cleaved@D175	5A1E	7.5	CST
174Yb	CK8/18	Total	C51	7.5	CST
175Lu	Pan-ACTIN	C-terminal domain	D18C11	7.5	CST

176Yb	H3	C-terminal domain	D1H2	7.5	CST
-------	----	-------------------	------	-----	-----

CST = Cell Signaling Technology, BD = Becton Dickinson. Community validation data for antibodies are given in Supplementary Note 1.

Supplementary Table 3 | Antibodies used for adherent cell imaging (Fig. 4).

Isotope	Antigen	Antibody raised against	Clone	Final conc. [$\mu\text{g/mL}$]	Supplier
139La	pCREB	pS133	J151-21	3.5	BD
141Pr	pSTAT5	pY694	47	3.5	BD
142Nd	pSHP2	pY542		3.5	Abcam
143Nd	p53	Total	7F5	3.5	CST
145Nd	TWIST	Amino-terminal residues	ABD29	3.5	Millipore
146Nd	ZEB1	Total	MAB6708	3.5	R&D Systems
147Sm	c-MYC	Amino-terminal residues	D84C12	3.5	CST
148Nd	SLUG	Total	C19G7	3.5	CST
150Nd	pNF κ B	pS529	K10-895.12.50	3.5	BD
151Eu	p38	pT180/ pY182	36/ p38	3.5	BD
152Sm	pAMPK	pT172	40H9	3.5	CST
153Eu	pAKT	pS473	D9E	3.5	CST
154Gd	pERK1/2	pT202/ pY204	20A	3.5	BD
156Gd	Double-stranded DNA	Double-stranded DNA	AE-2	3.5	Millipore
158Gd	pGSK3	pS9	D85E12	3.5	CST
159Tb	pSMAD2/3	pS465/pS467	D6G10	3.5	CST
160Gd	CD44	Total, surface	IM7	3.5	BD
162Dy	VIMENTIN	Total	RV202	3.5	BD
164Dy	pSMAD1/5/7	pS463/pS465	41D10	3.5	CST
165Ho	β -CATENIN	Total, when S33/S37/T41 are not phosphorylated	D13A1	3.5	CST
166Er	CAH IX	Total	AF2188	3.5	R&D Systems
167Er	E-CADHERIN	C-terminal residues	36/E-Cadherin	3.5	BD

168Er	CD24	Total, surface	ML5	3.5	BD
169Tm	pPLC γ 2	pY759	K86-689.37	3.5	BD
170Er	pH3	pS28	HTA28	3.5	Biologend
171Yb	pS6	pS235/pS236	N7-548	3.5	BD
172Yb	Cleaved PARP	Cleaved@D214	F21-852	3.5	BD
174Yb	Cleaved CASPASE3	Cleaved@D175	C92-605	3.5	BD

CST = Cell Signaling Technology, BD = Becton Dickinson. Community validation data for antibodies are given in Supplementary Note 1.

Supplementary Table 4 | Analyzed tumor samples.

HER2 FISH	Mol. Signature (IHC)	Tissue type	ID	Resolution	Tumor subtype	pT	pN	M	Grade	Multifocal_centric
Normal	Luminal (HER2 neg)	Primary tumor	79	1 µm	Invasive ductal	pT2	pN0 (sn)	0	G3	Unifocal
Normal	Luminal (HER2 neg)	Primary tumor	95	1 µm	Invasive ductal	pT2	pN1	0	G3	Multicentric/focal
Amplification	HER2 (non luminal)	Primary tumor	96*	1 µm	Invasive ductal	pT3	pN1	0	G3	Unifocal
Normal	Triple negativ	Primary tumor	162	1 µm	Invasive ductal	pT2	pN1	0	G3	Multicentric/focal
Amplification	HER2 (non luminal)	Primary tumor	199*	1 µm	Invasive ductal	pT2	pN1	1	G2	Unifocal
Normal	Triple negativ	Primary tumor	201	1 µm	Invasive ductal	pT1c		0	G2	Unifocal
Normal	Triple negativ	Primary tumor	201*	1 µm	Invasive ductal	pT1c		0	G2	Unifocal
Amplification	Luminal (HER2 pos)	Primary tumor	210	1 µm	Invasive ductal	pT1c	pN0	0	G2	Unifocal
Normal	Luminal (HER2 neg)	Primary tumor	254*	1 µm	Invasive cribriform	pT1c	pN0	0	G1	Unifocal
Amplification	Luminal (HER2 pos)	Primary tumor	257	1 µm	Invasive ductal	pT2	pN3	0	G3	Unifocal
Normal	Luminal (HER2 neg)	Tumor recurrence	260	2 µm	Invasive ductal	pT1c				
Normal	Luminal (HER2 neg)	Primary tumor	261	2 µm	Invasive ductal	pT1c	pN0 (sn)	0	G2	Unifocal
Amplification	HER2 (non luminal)	Primary tumor	273	1 µm	Invasive ductal	pT4	pN1	0	G3	Unifocal
Amplification	Luminal (HER2 pos)	Primary tumor	276	1 µm	Invasive ductal	pT2	pN3	0	G3	Unifocal
Normal	Luminal (HER2 neg)	Primary tumor	283	1 µm	Invasive ductal	pT1c	pN0	0	G2	Multicentric/focal
Normal	Luminal (HER2 neg)	Lymph node metastasis	290	2 µm	Invasive ductal					
Amplification	HER2 (non luminal)	Primary tumor	294*	1 µm	Invasive ductal	pT1c	pN0 (sn)	0	G3	Unifocal
Normal	Triple negativ	Primary tumor	304	1 µm	Invasive ductal	pT2	pN1	0	G3	Unifocal
Normal	Luminal (HER2 neg)	Tumor recurrence	321	1 µm	Invasive lobular					
Normal	Normal breast	Normal breast tissue	343*	1 µm						
Normal	Normal breast	Normal breast tissue	359*	1 µm						

Samples highlighted with a (*) were from TMA 2, samples without a (*) were from TMA 1. pT: Tumor; pN: Node; pM: Metastasis; pT1mic: microinvasion 0.1 cm or less in greatest dimension; pT1a: tumor more than 0.1 but not more than 0.5 cm in greatest dimension; pT1b: tumor more than 0.5 cm but not more than 1.0 cm in greatest dimension; pT1c: tumor more than 1.0 cm but not more than 2.0 cm in greatest dimension; pT2: tumor more than 2.0 cm but not more than 5.0 cm in greatest dimension; pT3: tumor more than 5.0 cm in greatest dimension; pT4: tumor of any size with direct extension to (a) chest wall or (b) skin; pN0: no regional lymph node metastases; pN1: micrometastases or metastases in one to three axillary lymph nodes and/or in internal mammary nodes with metastases detected

by sentinel lymph node biopsy but not clinically detected; pN2: metastases in four to nine axillary lymph nodes or in clinically detected internal mammary lymph nodes in the absence of axillary lymph node metastases; pN3: metastases in 10 or more axillary lymph nodes, or in infraclavicular (level III axillary) lymph nodes, or in clinically detected ipsilateral internal mammary lymph nodes in the presence of 1 or more positive level I or II axillary lymph nodes, or in more than 3 axillary lymph nodes and in internal mammary lymph nodes with micrometastases or macrometastases detected by sentinel lymph node biopsy but not clinically detected, or in ipsilateral supraclavicular lymph nodes; sn: sentinel lymph node biopsy; M0: no distant metastases found; M1: distant metastases; G: Grade 1-3 according to Nottingham Criteria.

Tissues no. 23 and no. 37 were of the Luminal HER2+ subtype and not part of a TMA.

Supplementary Table 5 | Antibodies used for tissue imaging (TMA 1).

Isotope	Antigen	Antibody raised against	Clone	Final conc. [$\mu\text{g/mL}$]	Supplier
139La	ER	Total, synthetic peptide within residues 200 - 300		7.5	Abcam
141Pr	PR	Residues surrounding Y541	D8Q2J	7.5	CST
142Nd	pSHP2	pY542		5	Abcam
143Nd	p53	Total	7F5	5	CST
144Nd	CD31	Total, surface	HC1/6	5	Millipore
145Nd	TWIST	Amino-terminal residues	ABD29	5	Millipore
146Nd	CD68	Total, surface	Y1/82A	7.5	Biolegend
147Sm	CD3	Total, surface	UCHT1	4.6	Biolegend
148Nd	SLUG	Total	C19G7	1	CST
149Sm	CD20	Total, surface	L26	5	eBioscience
150Nd	c-MYC	C-terminal domain	9 E10	7.5	Biolegend
151Eu	HER2	C-terminal domain	3B5	7.5	BD
152Sm	pAMPK	pT172	40H9	7.5	CST
153Eu	pAKT	pS473	D9E	1	CST
154Gd	pERK1/2	pT202/pY204	D13.14.4E	7.5	CST
156Gd	pNF κ B	pS536		7.5	Abcam
158Gd	pGSK3	pS9	5B3	5	CST
159Tb	pBAD	pS112	40A9	7.5	CST
160Gd	CD44	Total, surface	IM7	5	BD
162Dy	VIMENTIN	Total	D21H3	7.5	CST
164Dy	CK7	Total	RCK105	7.5	BD
165Ho	β -CATENIN	Total, when S33/S37/T41 are not phosphorylated	D13A1	7.5	CST
166Er	CAH IX	Total	AF2188	7.5	R&D Systems

167Er	E-CADHERIN	C-terminal residues	36/E-Cadherin	7.5	BD
168Er	Ki67	Total	B56	7.5	BD
169Tm	EGFR	Cytoplasmic domain	D38B1	7.5	CST
170Er	pS6	pS235/pS236	D57.2.2E	7.5	CST
171Yb	CD45	Total, surface	HI30	5	Biologend
172Yb	CASPASE3	Cleaved@D175	5A1E	5	CST
174Yb	CK8/18	Total	C51	7.5	CST
175Lu	Pan-ACTIN	C-terminal domain	D18C11	7.5	CST
176Yb	H3	C-terminal domain	D1H2	5	CST

CST = Cell Signaling Technology, BD = Becton Dickinson. Community validation data for antibodies are given in Supplementary Note 1.

Supplementary Table 6 | Antibodies used for tissue imaging (TMA 2).

Isotope	Antigen	Antibody raised against	Clone	Final conc. [$\mu\text{g/mL}$]	Supplier
139La	ER	Total, synthetic peptide within residues 200 - 300		7.5	Abcam
141Pr	PR	Residues surrounding Tyr541	D8Q2J	7.5	CST
142Nd	pSHP2	pY542		5	Abcam
143Nd	p53	Total	7F5	5	CST
144Nd	CD31	Total, surface	HC1/6	5	Millipore
145Nd	TWIST	Amino-terminal residues	ABD29	7.5	Millipore
146Nd	CD68	Total, surface	Y1/82A	7.5	Biolegend
147Sm	CD3	Total, surface	UCHT1	5	Biolegend
148Nd	SLUG	Total	C19G7	1.3	CST
149Sm	CD20	Total, surface	L26	5	eBioscience
150Nd	c-MYC	C-terminal domain	9 E10	7.5	Biolegend
151Eu	HER2	C-terminal domain	3B5	5	BD
152Sm	pAMPK	pT172	40H9	7.5	CST
153Eu	pAKT	pS473	D9E	1.3	CST
154Gd	pERK1/2	pT202/pY204	D13.14.4E	7.5	CST
156Gd	pNF κ B	pS536		7.5	Abcam
158Gd	pGSK3	pS9	5B3	5	CST
159Tb	pBAD	pS112	40A9	7.5	CST
160Gd	CD44	Total, surface	IM7	5	BD
162Dy	VIMENTIN	Total	D21H3	7.5	CST
164Dy	CK7	Total	RCK105	5	BD
165Ho	β -CATENIN	Total, when S33/S37/T41 are not phosphorylated	D13A1	7.5	CST
166Er	CAH IX	Total	AF2188	7.5	R&D Systems

167Er	E-CADHERIN	C-terminal residues	36/E-Cadherin	7.5	BD
168Er	Ki67	Total	B56	7.5	BD
169Tm	EGFR	Cytoplasmic domain	D38B1	7.5	CST
170Er	pS6	pS235/pS236	D57.2.2E	7.5	CST
171Yb	CD45	Total, surface	HI30	5	Biologend
172Yb	CASPASE3	Cleaved@D175	5A1E	5	CST
174Yb	CK8/18	Total	C51	7.5	CST
175Lu	Pan-ACTIN	C-terminal domain	D18C11	7.5	CST
176Yb	H3	C-terminal domain	D1H2	5	CST

CST = Cell Signaling Technology, BD = Becton Dickinson. Community validation data for antibodies are given in Supplementary Note 1.

SUPPLEMENTARY NOTES

Supplementary Note 1 | Example validations of the antibodies used in this study by the research community. The list is not exhaustive.

CD3: clone UCHT1, Biolegend, mass tag 147Sm

Pollard K, Lunny D, Holgate CS, Jackson P, Bird CC. Fixation, processing, and immunochemical reagent effects on preservation of t-lymphocyte surface membrane antigens in paraffin-embedded tissue. *J. Histochem. Cytochem.* 1987 Nov;35(11): 1329-1338. (Clone-specific: Immunohistochemistry)

CK7: clone RCK105, BD, mass tag 164Dy

Smedts F, Ramaekers F, Robben H, et al. Changing patterns of keratin expression during progression of cervical intraepithelial neoplasia. *Am. J. Pathol.* 1990; 136(3):657-668. (Clone-specific: Immunohistochemistry)

CD20: clone L26, eBioscience, mass tag 149Nd

Mason DY, Comans-Bitter WM, Cordell JL, Verhoeven MA, van Dongen JJ. Antibody L26 recognizes an intracellular epitope on the B-cell-associated CD20 antigen. *Am. J. Pathol.* 1990 Jun;136(6):1215-22. (Clone-specific: Immunohistochemistry)

CD45: clone HI30, Biolegend, mass tag 171Yb

Friedman T, Shimizu A, Smith RN, Colvin RB, Seebach JD, Sachs DH, Iacomini J. Human CD4+ T Cells Mediate Rejection of Porcine Xenografts. *J. Immunol.* 1999 May; 162(9): 5256-5262. (Clone-specific: Immunohistochemistry)

CD68: clone KP1, eBioscience, mass tag 146Nd

Horny HP, Schaumburg-Lever G, Bolz S, Geerts ML, Kaiserling E. Use of monoclonal antibody KP1 for identifying normal and neoplastic human mast cells. *J. Clin. Pathol.* 1990 Sep;43(9):719-22. (Clone-specific: Immunohistochemistry)

Pulford KA, Rigney EM, Micklem KJ, Jones M, Stross WP, Gatter KC, Mason DY. KP1: a new monoclonal antibody that detects a monocyte/macrophage associated antigen in routinely

processed tissue sections. J. Clin. Pathol. 1989 Apr;42(4):414-21. (Clone-specific: Immunohistochemistry)

c-MYC: clone 9E10, Biologend, mass tag 150Nd

Blancate J, Singh B, Liu A, Liao DJ, Dickson RB. Correlation of amplification and overexpression of the c-myc oncogene in high-grade breast cancer: FISH, in situ hybridization and immunohistochemical analyses. British Journal of Cancer 2004; 90: 1612-1619. (Clone-specific: Immunohistochemistry)

Cleaved Caspase-3 (Asp175): clone 5A1E, CST, mass tag 172Yb

Hokkanen S, Feldmann HM, Ding H, Jung C, Bojarski L, Renner-Müller I, Schüller U, Kretzschmar H, Wolf E, Herms J. Lack of Pur-alpha alters postnatal brain development and causes megalencephaly. Hum. Mol. Genet. 2012; 21(3):473-84. (Clone-specific: Immunohistochemistry)

Kash JC, Walters KA, Davis AS, Sandouk A, Schwartzman LM, Jagger BW, Chertow DS, Li Q, Kuestner RE, Ozinsky A, Taubenberger JK. Lethal synergism of 2009 pandemic H1N1 influenza virus and Streptococcus pneumoniae coinfection is associated with loss of murine lung repair responses. MBio. 2011; 2(5) pii: e00172-11. (Clone-specific: Immunohistochemistry)

EGF Receptor: clone D38B1, CST, mass tag 169Tm

Kawahara A, Yamamoto C, Nakashima K, Azuma K, Hattori S, Kashihara M, Aizawa H, Basaki Y, Kuwano M, Kage M, Mitsudomi T, Ono M. Molecular diagnosis of activating EGFR mutations in non-small cell lung cancer using mutation-specific antibodies for immunohistochemical analysis. Clin. Cancer Res. 2010; 16(12):3163-70. (Clone-specific: Immunohistochemistry)

E-Cadherin: clone 36/E-Cadherin, BD, mass tag 167Er

Miyoshi K, Shillingford JM, Smith GH, et al. Signal transducer and activator of transcription (Stat) 5 controls the proliferation and differentiation of mammary alveolar epithelium. J. Cell. Biol. 2001; 155(4):531-542. (Clone-specific: Immunohistochemistry)

HER2/c-ErbB-2: clone 3B5, BD, mass tag 151Eu

Martinazzi M, Crivelli F, Zampatti C, Martinazzi S. Relationships between epidermal growth factor receptor (EGF-R) and other predictors of prognosis in breast carcinomas. An

immunohistochemical study. *Pathologica*. 1993; 85(1100):637-644. (Clone-specific: Immunohistochemistry)

Meissner K, Riviere A, Haupt G, Loning T. Study of neu-protein expression in mammary Paget's disease with and without underlying breast carcinoma and in extramammary Paget's disease. *Am. J. Pathol.* 1990; 137(6):1305-1309. (Clone-specific: Immunohistochemistry)

Penault-Llorca F, Adelaide J, Houvenaeghel G, Hassoun J, Birnbaum D, Jacquemier J. Optimization of immunohistochemical detection of ERBB2 in human breast cancer: impact of fixation. *J. Pathol.* 1994; 173(1):65-75. (Clone-specific: Immunohistochemistry)

Schwechheimer K, Laufle RM, Schmahl W, Knodlseder M, Fischer H, Hofler H. Expression of neu/c-erbB-2 in human brain tumors. *Hum Pathol.* 1994; 25(8):772-780. (Clone-specific: Immunohistochemistry)

Singleton TP, Niehans GA, Gu F, et al. Detection of c-erbB-2 activation in paraffin-embedded tissue by immunohistochemistry. *Hum. Pathol.* 1992; 23(10):1141-1150. (Clone-specific: Immunohistochemistry)

van de Vijver MJ, Peterse JL, Mooi WJ, et al. Neu-protein overexpression in breast cancer. Association with comedo-type ductal carcinoma in situ and limited prognostic value in stage II breast cancer. *N. Engl. J. Med.* 1988; 319(19):1239-1245. (Clone-specific: Immunohistochemistry, Immunoprecipitation)

Zhau HE, Zhang X, von Eschenbach AC, et al. Amplification and expression of the c-erb B-2/neu proto-oncogene in human bladder cancer. *Mol. Carcinog.* 1990; 3(5):254-257. (Clone-specific: Immunohistochemistry, Western blot)

p53: clone 7F5, CST, mass tag 143Nd

Li LP, Cheng WB, Li H, Li W, Yang H, Wen DH, Tang YD. Expression of proteasome activator REGγ in human laryngeal carcinoma and associations with tumor suppressor proteins. *Asian Pac. J. Cancer Prev.* 2012;13(6):2699-703. (Clone-specific: Immunohistochemistry)

pAkt (Ser473): clone D9E, CST, mass tag 153Eu

Engelman JA, Chen L, Tan X, Crosby K, Guimaraes AR, Upadhyay R, Maira M, McNamara K, Perera SA, Song Y, Chirieac LR, Kaur R, Lightbown A, Simendinger J, Li T, Padera RF, García-Echeverría C, Weissleder R, Mahmood U, Cantley LC, Wong KK. Effective use of PI3K and MEK inhibitors to treat mutant Kras G12D and PIK3CA H1047R murine lung cancers. *Nat Med.* 2008;14(12):1351-6. (Clone-specific: Immunohistochemistry)

Guertin DA, Stevens DM, Saitoh M, Kinkel S, Crosby K, Sheen JH, Mullholland DJ, Magnuson MA, Wu H, Sabatini DM. mTOR complex 2 is required for the development of prostate cancer induced by Pten loss in mice. *Cancer Cell.* 2009;15(2):148-59. (Clone-specific: Immunohistochemistry)

pAMPK α (Thr172): clone 40H9, CST, mass tag 152Sm

Nakada Y, Stewart TG, Peña CG, Zhang S, Zhao N, Bardeesy N, Sharpless NE, Wong KK, Hayes DN, Castrillon DH. The LKB1 tumor suppressor as a biomarker in mouse and human tissues. *PLoS One.* 2013 Sep 25;8(9). (Clone-specific: Immunohistochemistry)

pBad (Ser112): clone 40A9, CST, mass tag 159Tb

Holzer TR, Fulford AD, Arkins AM, Grondin JM, Mundy CW, Nasir A, Schade AE. Ischemic time impacts biological integrity of phospho-proteins in PI3K/Akt, Erk/MAPK, and p38 MAPK signaling networks. *Anticancer Res.* 2011 Jun;31(6):2073-81. (Clone-specific: Immunohistochemistry)

pERK1/2 (Thr202/Tyr204): clone D13.14.4E, CST, mass tag 154Gd

Engelman JA, Chen L, Tan X, Crosby K, Guimaraes AR, Upadhyay R, Maira M, McNamara K, Perera SA, Song Y, Chirieac LR, Kaur R, Lightbown A, Simendinger J, Li T, Padera RF, García-Echeverría C, Weissleder R, Mahmood U, Cantley LC, Wong KK. Effective use of PI3K and MEK inhibitors to treat mutant Kras G12D and PIK3CA H1047R murine lung cancers. *Nat Med.* 2008;14(12):1351-6. (Clone-specific: Immunohistochemistry)

pGSK-3 β (Ser9): clone 5B3, CST, mass tag 158Gd

Guertin DA, Stevens DM, Saitoh M, Kinkel S, Crosby K, Sheen JH, Mullholland DJ, Magnuson MA, Wu H, Sabatini DM. mTOR complex 2 is required for the development of prostate cancer induced by Pten loss in mice. *Cancer Cell.* 2009;15(2):148-59. (Clone-specific: Immunohistochemistry)

Vimentin: clone D21H3, CST, mass tag 162Dy

Park J, Morley TS, Scherer PE. Inhibition of endotrophin, a cleavage product of collagen VI, confers cisplatin sensitivity to tumours. *EMBO Mol. Med.* 2013, 5(6):935-48. (Clone-specific: Immunohistochemistry)

Supplementary Note 2 | Patient classification by SPADE

The SPADE analysis partly reflected the tumor subtypes as can be seen in Figure 5. Yet, the ability of SPADE to accurately reflect the breast cancer subtypes in our setting is limited. E.g. the high number of markers that have been used for clustering step will generate many more cell subpopulations than the existing sub-types and the identified cell subpopulations will depend on the imaged area (see discussion in the main text). Therefore some cell subpopulations from each patient (e.g. immune cells present vs. not present) will be found in different parts of the SPADE tree, depending on the imaged area. Also, although certain cell clusters are close in the high dimensional space, they do not necessarily appear so in the two-dimensional representation. Furthermore, SPADE generates different minimum spanning tree representations every time it is run on the same data-set, mainly due to the agglomerative clustering and minimum spanning tree construction steps that may or may not yield a representation of the current breast cancer classification. These thoughts should not distract from the fact, that SPADE is a powerful visualization tool for high dimensional single-cell data that allows to manually assign cell subpopulations and therefore to delineate a map of breast cancer cell subpopulations as done in this publication.

Supplementary Note 3 | Single-cell segmentation

In general, single-cell segmentation of tissue images is a challenging task due to several reasons: First, in 5- μm thick tissue sections a small percentage of cells will lie over each other, second, some cells are only partially represented, third, cells can be too close to each other to be segmented, and fourth, small differences in the position of the segmentation line can lead to spill-over of signal from one to another cell. This is a challenge common to all tissue analysis approaches that rely on tissue image segmentation, including IMC, IHC, and IFM approaches. Therefore care must be taken when small side-populations with “new” marker combinations are detected based on tissue based segmentation analyses. To reduce these errors by the used watershed algorithm, we manually corrected the cell segmentation masks.